Comparison of Fluorine-18-Fluorodeoxyglucose PET, MRI and Endoscopy for Staging Head and Neck Squamous-Cell Carcinomas

C. Laubenbacher, D. Saumweber, C. Wagner-Manslau, R. J. Kau, M. Herz, N. Avril, S. Ziegler, C. Kruschke, W. Arnold and M. Schwaiger

Departments of Nuclear Medicine and Otorhinolaryngology, Technical University of Munich, Munich, Germany

Accurate, preoperative assessment of tumor extent and lymph node involvement is mandatory for individualized therapy in patients with squamous-cell carcinomas (SCCs) of the head and neck region. Metabolic imaging, [^{18}F]fluorodeoxyglucose (FDG) PET and MRI were compared with postoperative, histologic tissue characterization. **Methods:** Dynamic and static PET with 370 MBq [^{18}F]FDG up to 60 min postinjection and MRI were compared prospectively in 22 patients with head and neck SCCs. PET results with and without attenuation correction were compared with postoperative T and N stages based on pathologic findings. **Results:** Kinetic characteristics and tracer uptake intensity were similar in primary tumors and lymph node metastases. In both, FDG uptake did not reach a plateau phase 60 min postinjection. There was no statistically significant correlation of FDG uptake with plasma glucose level or histologic grading. All primary tumors were clearly demonstrated by PET, which tended to overestimate tumor size. The sensitivity and specificity for detecting individual lymph node involvement were 90% and 96%, respectively, for PET and, thus, significantly higher for MRI (78% and 71%, respectively; $p < 0.05$). N stages were correctly identified by MRI in only 4 patients; PET correctly staged lymph nodes in 15 of 17 patients. Based on "neck sides," the sensitivity and specificity were higher for PET, 89% and 100%, respectively, compared with MRI values of 72% and 56%, respectively. **Conclusion:** FDG-PET may be helpful in detecting occult primary tumors with positive lymph nodes.

Key Words: positron emission tomography; fluorine-18-flurodeoxyglucose; magnetic resonance imaging; squamous-cell carcinoma

J Nucl Med 1995; 36:1747–1757

The incidence of squamous-cell carcinomas (SCCs) of the upper aerodigestive tract is increasing (*1*). Unfortunately, advanced tumor stages prevail at the time of first diagnosis. Although chemotherapy and radiation therapy often are used in the treatment of patients with SCCs of the head and neck, the most common therapeutic regimen is still surgical resection. The success of surgical therapy depends on radical elimination of the primary tumor and involved lymph nodes. For planning surgical strategy (type of neck dissection) and deciding whether postsurgical treatment (radiochemotherapy) is necessary, accurate preoperative tumor-node-metastasis (TNM) staging of SCCs is mandatory. Previously, only morphologic procedures such as sonography, CT or MRI were used for staging; however, the morphologic parameters provided by these procedures are of limited specificity in delineating lymph node involvement by the tumor.

Metabolic parameters, which are independent of morphologic changes, are expected to improve the accuracy of preoperative TNM staging. Uptake of radiolabeled substrates such as glucose or amino acids in tumor tissue can be used as diagnostic tools. Almost 50 yr ago, Warburg (*2*) and Warburg et al. (*3*) documented increased glycolysis in tumors. Recently, it has become possible to assess regional metabolism noninvasively with PET and metabolic tracers. By using [^{18}F]FDG, a glucose analog, PET allows the noninvasive study of glucose metabolism in humans (*4*). FDG-PET has been successfully applied to a variety of malignant human tumors, such as brain tumors (*5–12*), lung tumors (*13,14*), musculoskeletal tumors (*15*), pancreatic cancer (*16*) and breast carcinomas (*17,18*). Reisser et al. (*19*), Haberkorn et al. (*20,21*), Jabour et al. (*22*), and Lindholm et al. (*23*) previously demonstrated that SCCs of the head and neck have increased FDG uptake.

The purpose of this study was to answer three clinically relevant questions:

1. Is there a correlation between quantitatively assessed FDG uptake in primary tumors and histologic grading?
2. Does [^{18}F]FDG PET increase the diagnostic accuracy of preoperative assessment of primary tumor and lymph node status in patients with SCCs of the head and neck?
3. Is attenuation correction necessary for detection and staging of head and neck tumors by PET?

Received Aug. 15, 1994; revision accepted Feb. 14, 1995.

For correspondence or reprints contact: C. Laubenbacher, MD, Nuklearmedicine Clinic, Technical University of Munich, Klinikum rechts der Isar, Ismaningerstr. 22, D-81675 Munich, Germany.

TABLE 1
Uptake in Primary Tumors (n = 22) and Lymph Node Metastases (n = 41)

Patient no. (n = 22)	Sex	Age	Location	Stage T	Stage N	Stage G	SUV tumor (n = 22)	SUV lymph node metastases (n = 41)
1	M	56	Hypo	4	2b	4	8.9	8.9, 11.4
2*	F	59	Oro				6.4	7.9, 5.3
								5.6, 8.6
3	M	61	Hypo	2	2c	3	5.7	6.7, 5.6
								5.6, 4.4
4	M	47	Oro	1	2b	3	4.9	5.2, 4.8, 3.6
5	M	56	Oro	2	1	3	13.8	—
6*	M	53	Hypo				8.0	4.8, 3.4
7*	M	70	Oro				5.1	3.7, 5.1
								4.2, 4.7
8	M	41	Hypo	3	2c	2	2.0	1.4
9*	M	50	Oro				7.2	9.3, 8.2, 4.3
10	M	42	Hypo	2	2b	2	2.3	2.0, 1.9
11	M	57	Hypo	1	2b	3	5.9	5.7, 7.2
								7.8, 8.0
12	M	54	Oro	1	0	4	3.3	—
13	M	52	Oro	1	1	2	2.3	—
14	M	65	Hypo	3	2b	2	8.4	3.5
15	M	53	Oro	1	2b	2	2.5	3.2, 6.8
16*	M	61	Oro				3.4	6.5
17	M	38	Oro	4	3	3	8.3	5.9, 2.9
18	F	56	Oro	2	1	2	5.1	—
19	M	53	Oro	3	2b	3	7.3	4.3, 1.8
20	M	65	Oro	2	1	3	6.4	2.1
21	M	54	Hypo	2	0	4	12.8	—
22	M	54	Hypo	2	2b	3	9.1	9.1, 5.9, 4.3
Mean ± s.d.		54.4 ± 7.8	Oro: 13×				6.3 ± 3.2	5.4 ± 2.3
Range		38–70	Hypo: 9×				2.0–13.8	1.4–11.4

*Patients who did not undergo surgery.
Hypo = hypopharynx; Oro = oropharynx; SUV = standardized uptake value.

MATERIALS AND METHODS

Patients

We studied 22 consecutive patients (20 men, 2 women; aged 38–70 yr; mean body weight 68.7 ± 12.7 kg; mean height 170 ± 8.5 cm) diagnosed with head and neck SCCs, as determined by biopsy, who were referred to the Department of Otorhinolaryngology for surgery (Table 1). Exclusion criteria were prior treatment, known diabetes mellitus or possible pregnancy. All patients underwent preoperative endoscopy, MRI and [^{18}F]FDG PET within 2 wk of surgery. Informed written consent was obtained from all patients.

PET

All patients were studied after an overnight fast. Before PET, the patient's plasma glucose level was measured with a standard clinical test.

Patients were positioned on a 31-slice whole-body PET scanner, which has 16 circular detector rings to allow simultaneous acquisition of 31 contiguous transaxial images with a slice separation of 3.375 mm. PET images were generated using filtered backprojection and corrected for decay. The reconstructed in-plane image resolution was 7 mm FWHM, and the axial resolution was 5 mm FWHM.

Fluorodeoxyglucose was produced by a method modified from the synthesis of Hamacher et al. (*24*). The radiochemical purity was measured with high-performance liquid chromatography; values above 98% were found.

Before emission scanning, transmission scans were obtained for 20 min over the tumor region, which yielded more than 4 million counts per slice. Patients were intravenously injected with 370 MBq [^{18}F]FDG, and dynamic emission scans were obtained (6 × 5 min or 3 × 10 min). Subsequently, static emission scans in two or three contiguous bed positions were obtained; each bed position encompassed a 10.8-cm axial field view. A schematic display of the PET protocol is shown in Figure 1. In the first bed position, over the tumor region, PET images were corrected for attenuation. For quantitative evaluation, regions of interest were defined over areas with increased FDG uptake (tumor and lymph node metastases). Regional FDG uptake was expressed as the standardized uptake value (SUV).

$$\text{SUV} = \frac{\text{decay-corrected tissue concentration}}{\text{injected dose (in nanocuries)/}}$$

$$\frac{\text{(in nanocuries per gram)in tumors or metastases}}{\text{body weight (in grams)}}.$$

According to Haberkorn et al. (*21*), lymph node involvement was defined as SUV > 2.0 or, in nonattenuation-corrected images

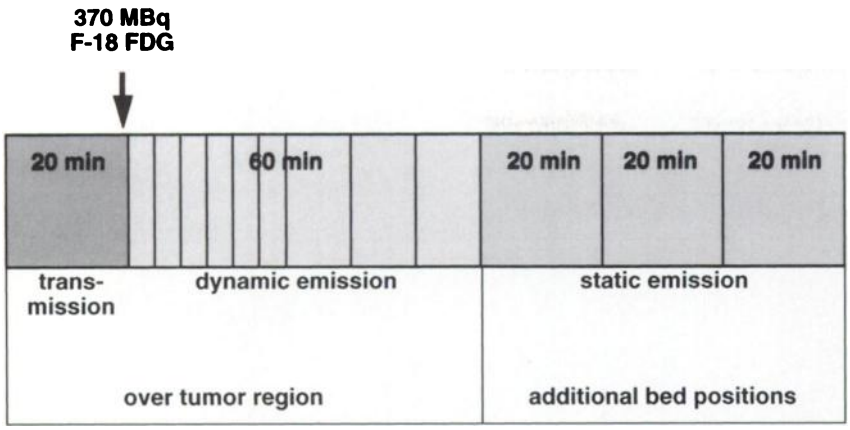

FIGURE 1. Protocol of [^{18}F]FDG PET examination in patients with head and neck SCC. After 20-min transmission scanning, dynamic emission scanning (6 × 5 min, 3 × 10 min) was performed over the tumor region. Two (three) additional bed positions were added to cover the whole head and neck region to assess lymph node status.

(additional static emission scans), as the target-to-nontarget ^{18}F activity ratio > 2.0.

Although T staging of primary tumors is based on anatomic information, we evaluated tumor extension in neighboring anatomic structures by comparing PET images with anatomic maps and normal FDG distribution in the head and neck region, as described by Jabour et al. (*22*).

MRI

MRI was performed on a Philips (Hamburg, Germany) Gyroscan (1.5 Tesla). All patients had 24 transversal T1-weighted slices before and after intravenous contrast media [0.1 mmole of gadolinium diethylenetriaminepenta-acetic acid (Gd-DTPA)/kg body weight], proton- and T2-weighted images [repetition time (TR) in milliseconds per echo time (TE) in milliseconds of 600/20; 2000/80/120]. In addition, 15 coronal slices were obtained in the inversion recovery (IR) mode (TR 1400 msec, TE 30 msec, inversion time (TI) 120 msec). Results were coded according to the TNM classification (*25*) by an experienced radiologist. Lymph nodes were classified as positive if their largest dimension was larger than 1.5 cm.

Endoscopy

All patients underwent preoperative endoscopy within 1 wk before surgery. During this procedure, biopsy samples were taken for preoperative histopathologic examination. Endoscopy was done by an experienced ear, nose and throat (ENT) surgeon, who also performed the surgery. Endoscopic findings were classified preoperatively according to the TNM classification.

Histopathologic Examination

The localization of dissected tissue was documented by the surgeon to allow correlation between histologic findings and preoperative imaging results. After the specimens were embedded in paraffin, routine staining was performed. The size of primary tumors and lymph node metastases was measured in three dimensions. Under the assumption of a rotation ellipsoid, tumor and lymph node volume was calculated as follows:

$$V = \frac{\pi}{6} \cdot A \cdot B \cdot C,$$

with A, B and C indicating the three dimensions (*26*). Tumor and lymph node status were coded according to the TNM classification. In addition, differentiation of the primary tumors was graded as four groups (G1 to G4: G1, well; G2, moderately; G3, poorly differentiated; G4, anaplastic), as given by Hermanek and Sobin (*25*).

The results of preoperative examinations were compared with histopathologic classification, which served as the gold standard.

Statistical Analysis

Values are given as mean ± s.d. Data were expressed in terms of sensitivity and specificity and positive and negative predictive values. A Student's t-test with Bonferroni's correction was used to compare continuous variables in the groups, and noncontinuous variables were compared with Fisher's exact test or a chi square test, depending on sample sizes. Statistical significance was defined as p values ≤ 0.05.

RESULTS

Nine primary tumors were located in the hypopharynx and 13 in the oropharynx. Based on the various test results, 5 patients (patients 2, 6, 7, 9 and 16) were thought to have inoperable primary tumors and were referred for radiation therapy. No histopathologic data are available for these patients.

FDG

Extent of FDG Uptake. All primary tumors were clearly visualized by PET. Figure 2 shows the transverse, saggittal and coronal nonattenuation-corrected images of patient 17 who had SCC of the oropharynx. The coronal view clearly demonstrates multiple cervical lymph nodes with high FDG uptake on the right side. In addition, one single lesion is visualized on the contralateral side. All right-sided lesions were also seen on coronal MRI scans in the IR mode. The contralateral, histologically proved lymph node metastasis with a diameter of 1 cm was not reported to be suspicious in the MRI report.

FDG uptake was calculated for each tumor or lymph node in the attenuation-corrected bed position in a sum image, which consisted of frames 7 to 9 (31–60 min postinjection). The SUV in the primary tumor ranged from 2.0 to 13.8, with a mean value of 6.3 ± 3.2. In attenuation-corrected images, a total of 41 lymph nodes in 17 patients could be detected. The SUV in lymph nodes ranged from 1.4 to 11.4 (mean 5.4 ± 2.3). There was no statistically significant difference between the SUV values in primary

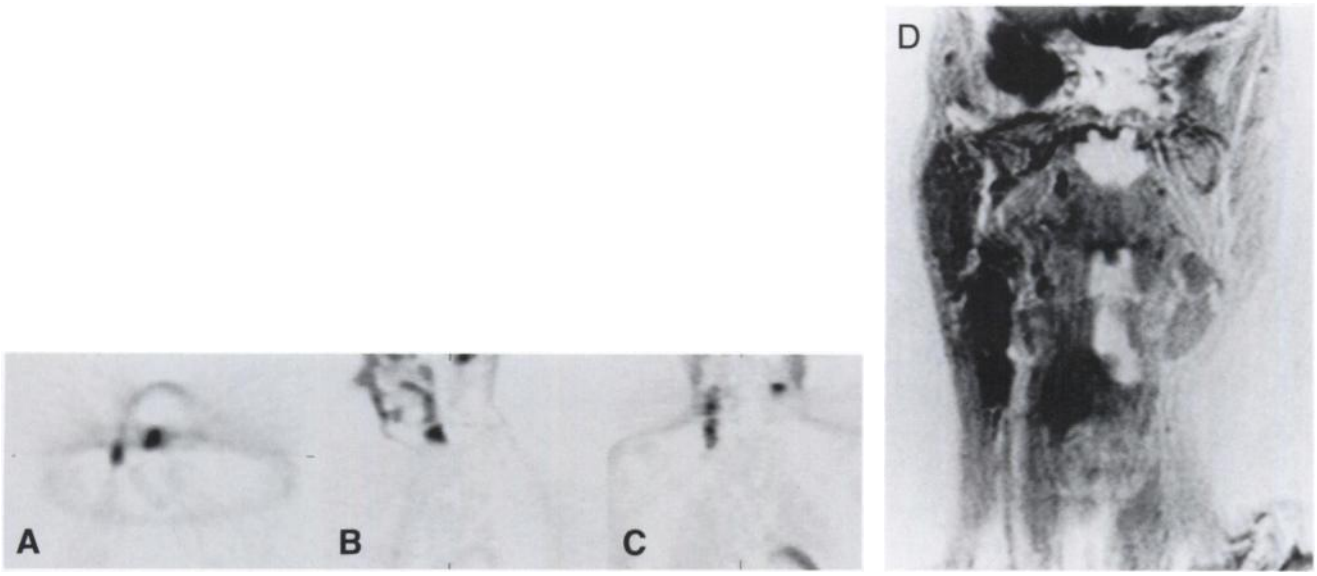

FIGURE 2. Static PET images without attenuation correction in transverse (A), sagittal (B) and coronal (C) views demonstrate high FDG uptake within SCCs of the oropharynx and in multiple cervical lymph nodes on the right side. A single, left-sided lesion with high FDG uptake is seen on the contralateral side. This histologically proven lymph node metastasis was not reported as suspicious on corresponding MR! scans in IR mode (D).

tumors and lymph node metastases (p = 0.24). In 17 patients, a correlation between the SUV of the primary tumor and the lymph node metastases in the same patient was possible (Fig. 3). Overall, there was no statistically significant correlation between these two parameters (p = 0.07). We found that patients with high FDG uptake in the primary tumors were likely to show high SUV values in their lymph node metastases. In the same patients, however, marked differences between individual lymph nodes were detected (e.g., in Patient 9, SUV of the primary tumor was 7.2 and SUV of the lymph nodes were 9.3, 8.2 and 4.3). There was also no significant relationship between the primary tumor site and FDG uptake [p = 0.42; SUV oropharynx (n = 13): 5.8 ± 3.1; SUV hypopharynx (n = 9): 7.0 ± 3.4].

Time Course of FDG Uptake. FDG uptake in tumor tissue and lymph node metastasis was calculated for each time frame. For better comparison between individuals, the SUV determined in the last frame (51–60 min) was set to 100% for normalization. The time course of FDG uptake in tumors and lymph node metastases are compared in Figure 4. Both curves demonstrate similar slopes. There was no statistically significant difference of SUV values for any time frame. FDG uptake did not reach a plateau phase 60 min postinjection.

Effect of Glucose Plasma Levels. After an overnight fast, glucose plasma levels determined before FDG injection were 5.1 ± 1.5 m*M*. In this group that had no known diabetic patients, there was no correlation between glucose plasma levels and FDG uptake of primary tumors (p = 0.94) or of lymph node metastases (p = 0.98) (Fig. 5).

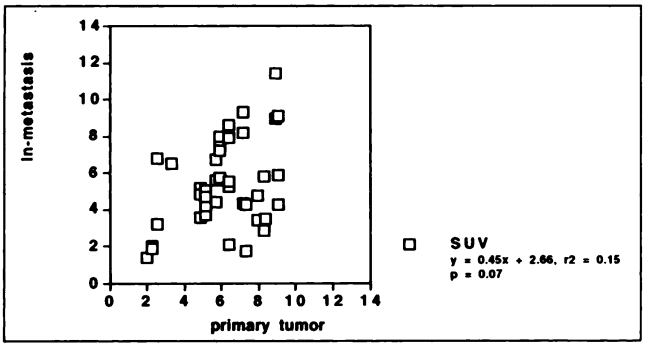

FIGURE 3. Correlation between SUV of primary tumors and lymph node metastasis in 17 patients. There is no statistically significant correlation between the two parameters (p = 0.07), but there seems to be a tendency for higher SUVs in lymph node metastases in patients with higher SUVs in primary tumors.

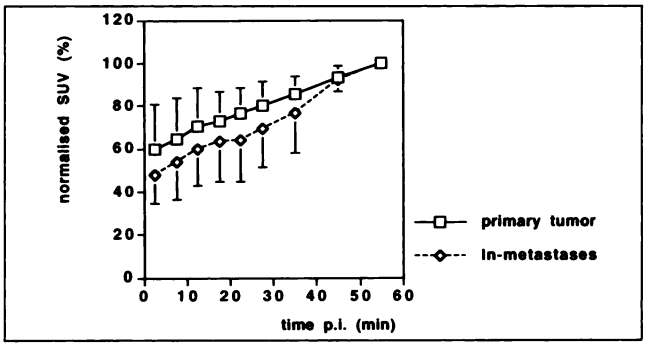

FIGURE 4. Time course of [^{18}F]FDG accumulation in primary tumors (n = 22) and lymph node metastases (n = 41) in patients with SCCs of the head and neck region.

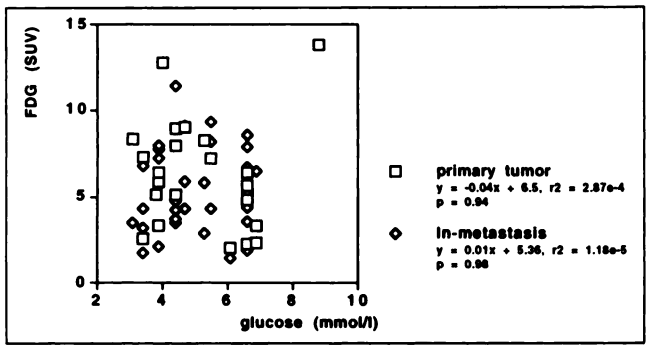

FIGURE 5. Fluorine-18 FDG uptake and plasma glucose levels in patients with SCCs of head and neck (22 primary tumors, 41 lymph node metastases). There is no correlation between the two parameters.

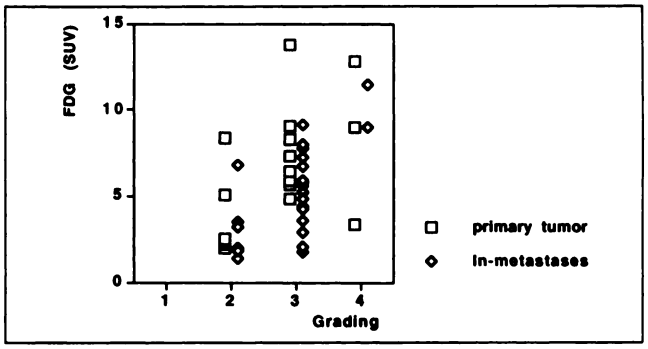

FIGURE 7. Correlation of postoperative histologic grading and standardized [^{18}F]FDG uptake in primary tumors (n = 17) and lymph node metastases (n = 27) of surgical patients with head and neck SCCs.

Effect of Lesion Size. The volume of the primary tumor and lymph node metastases was determined postoperatively, as described above. The volume of 17 primary tumors was 6.9 ± 6.0 ml (range 1.0–22.2 ml); the volume of 27 lymph node metastases was 15.6 ± 17.9 ml (range 1.4–80.1 ml). Only lymph node metastases that could be clearly identified by PET were correlated with surgical findings. FDG uptake and lesion volume were compared, as shown in Figure 6. There was no statistically significant correlation between these two parameters (volume of primary tumor compared with SUV, p = 0.09; volume of lymph node metastases compared with SUV, p = 0.20). There were eight primary tumors and eight lymph node metastases with a volume smaller than 5.0 ml. After analyzing only these small lesions, we could not detect a statistically significant correlation between SUV and lesion size for the primary tumors (p = 0.59) or lymph node metastases (p = 0.48). There was also no statistically significant correlations if tumor and lymph nodes were examined together (n = 16, p = 0.43).

Therapeutic Course. The therapeutic regimen (surgery or primary radiotherapy and type of neck dissection) was decided by an interdisciplinary conference with experienced ENT surgeons, oncologists and radiation therapists. Based on imaging results, five patients (2, 6, 7, 9 and 16) were thought to have inoperable primary tumors and were referred for radiation therapy. Seventeen of 22 patients had operable lesions and underwent surgery within 2 wk after PET. In these patients, all data concerning histopathologic classification could be obtained (1 woman and 16 men, age 53.2 ± 7.6, range 38.1–65.0). Eight of these tumors were in the hypopharynx and nine in the oropharynx. Except for Patient 12, who had a tumor on the floor of the mouth and underwent conservative ipsilateral neck dissection, all other patients had radical neck dissection on the side of the tumor. All patients with carcinomas located in the oropharynx also underwent ipsilateral suprahyoidal neck dissection. In 10 patients, contralateral conservative neck dissection was also performed. The decision of whether contralateral neck dissection was necessary was made by the ENT surgeon, after evaluating the results of all preoperative imaging modalities. For ethical reasons, the PET results were known to the surgeon preoperatively.

FDG Uptake and Grading

In the 17 patients who had surgery, there were six G2, eight G3 and three G4 carcinomas. With PET, we were able to correlate grading and SUV in all 17 primary tumors and in 27 lymph node metastases in these patients. Figure 7 shows the correlation between FDG uptake and histopathologic grading of the primary tumor and the lymph node metastases. There were no significant differences between mean SUV values for the different grading groups in primary tumors or in lymph node metastases. In the lymph node metastases group, however, the difference in the mean values between (1) G2 and G4 and (2) G3 and G4 would have been significant without Bonferroni correction,

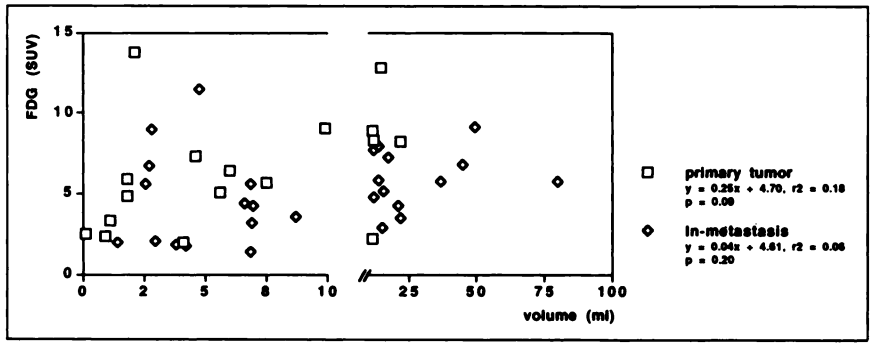

FIGURE 6. Correlation between [^{18}F]FDG uptake (SUV) and lesion volume in patients with head and neck SCCs (17 primary tumors, 27 lymph node metastases). Volumes were determined postoperatively in all tumors and in 27 lymph node metastases, in which definitive correlation between PET images and surgical specimen was possible.

which demonstrated a tendency to higher SUV values with decreasing differentiation.

T Staging

For preoperative staging, MRI, endoscopy and [^{18}F]FDG PET results were compared. These modalities and postoperative histopathologic examination were used to code tumor extent according to the TNM classification (*25*). Tumor staging mainly depends on the assessment of anatomic information, e.g., involvement of neighboring anatomic structures. Again, postoperative histopathologic examination served as the gold standard. Of the 17 patients who had surgery, 5 had T1, 7 T2, 3 T3 and 2 T4 tumors (Table 2). All tumors were clearly visualized by all three modalities. Endoscopy provided the best results, with correct tumor staging in 10 of 17 patients. Both MRI and PET correctly staged only seven patients and overstaged about one half of the patients.

N Staging

Preoperative lymph node status was assessed by MRI and [^{18}F]FDG PET. In the 17 patients who had surgery, 521 (15.9%) examined lymph nodes were malignant.

There were two patients with no lymph node involvement (stage N0: n = 2) and four patients with only one ipsilateral lymph node with a diameter less than 3.0 cm (N1: n = 4). In 11 patients with multiple malignant lymph nodes, 8 had only ipsilateral lymph node involvement (N2b: n = 8) and 2 also had malignant lymph nodes contralaterally (N2c: n = 2). One patient had a lymph node metastasis with a diameter greater than 6.0 cm (N3: n = 1) (Table 2). In 17 patients with 34 neck sides, 18 sides had malignant lymph node involvement.

Based on individual lymph nodes, PET correctly identified 75 of 83 (90.4%) histologically proven malignant lymph node. Nineteen of 438 (4.3%) benign lymph nodes had increased FDG uptake as a result of inflammatory reactions and therefore were classified as false-positive by PET. MRI had a sensitivity of 78% in correctly identifying 65 of 83 (78.3%) malignant lymph nodes. Because of reactive enlargement, 126 of 438 (28.8%) benign lymph nodes were misinterpreted as malignant, which resulted in a specificity of 71% (Table 3).

MRI also correctly identified lymph node involvement in only four patients. Eight patients were believed to have higher N stages and five to have a lower N stage. Two patients were falsely thought to have bilateral malignant lymph nodes. Overall, only 22 of 34 neck sides were correctly classified for lymph node involvement by MRI. In PET, there were only two false-negative classifications because of small ipsilateral lymph nodes with diameters of

TABLE 2
Endoscopy, MRI and Fluorine-18-FDG PET Results in Assessing Lymph Node Metastases and Tumor Staging in 17 Patients*

N staging	Histology	MRI	PET
Nodal metastases			
N0	2	2	4
N1	4	3	2
N2a	0	1	0
N2b	8	6	8
N2c	2	2	2
N3	1	3	1

	Correctly staged	Overstaged	Understaged
MRI	4/17	8/17	5/17
PET	15/17	0/17	2/17

T staging	Histology	Endoscopy	MRI	PET
Primary tumor				
T0	0	0	0	0
T1	5	0	1	2
T2	7	13	6	6
T3	3	1	5	8
T4	2	3	5	1

	Correctly staged	Overstaged	Understaged
MRI	7/17	10/17	0/17
PET	7/17	8/17	2/17
Endoscopy	10/17	6/17	1/17

*Postoperative histology was the gold standard.

TABLE 3
Estimates of Sensitivity, Specificity and Positive and Negative Predictive Values

		Lymph node metastases: Yes		Lymph node metastases: No			
PET	Positive	TP	75	FP	19	94	PPV 80%
	Negative	FN	8	TN	419	427	NPV 98%
			83		438	521	
		sens	90%	spec	96%		
MRI	Positive	TP	65	FP	126	191	PPV 34%
	Negative	FN	18	TN	312	330	NPV 95%
			83		438	521	
		sens	78%	spec	71%		

		Neck side with lymph node metastases: Yes		Neck side with lymph node metastases: No			
PET	Positive	TP	16	FP	0	16	PPV 100%
	Negative	FN	2	TN	16	18	NPV 89%
			18		16	34	
		sens	89%	spec	100%		
MRI	Positive	TP	13	FP	7	20	PPV 65%
	Negative	FN	5	TN	9	14	NPV 64%
			18		16	34	
		sens	72%	spec	56%		

*Seventeen patients (34 neck sides) with postoperative histopathological examination, which served as gold standard, were included.

TP = true-positive; FP = false-positive; FN = false-negative; TN = true-negative; PPV = positive predictive value; NPV = negative predictive value; sens = sensitivity; spec = specificity.

TABLE 4
Comparison of FDG Uptake of Squamous-Cell Carcinomas

Reference	No.	SUV		Plasma glucose level (mean ± s.d.)	Plasma insulin level (mean ± s.d.)
		Mean ± s.d.	Range		
Primary tumors					
Haberkorn et al. (*20*)	23*	3.2 ± 0.8	2.3–4.7	n.g.†	n.g.
Haberkorn et al. (*21*)	12‡	3.1 ± 1.1	2.0–5.9	n.g.	n.g.
Lindholm et al. (*23*)	5§	8.10 ± 2.05	5.6–10.9	5.4 ± 0.4	6.6 ± 3.0
	5¶	4.4 ± 1.0	3.3–5.9	10.0 ± 1.7	56.6 ± 14.9
This study	22¶	6.3 ± 3.2	2.0–13.8	5.1 ± 1.5	n.d.
Lymph node metastases					
Haberkorn et al. (*20*)	4*	3.3 ± 1.2	2.3–4.6	n.g.†	n.g.
Haberkorn et al. (*21*)	9**	3.2 ± 1.2	2.1–5.6	n.g.	n.g.
Lindholm et al. (*23*)	3§	5.0 ± 1.2	4.1–6.3	5.4 ± 0.4	6.6 ± 3.0
	3¶	3.4 ± 1.0	2.2–4.2	10.0 ± 1.7	56.6 ± 14.9
This study	41¶	5.1 ± 2.3	1.4–11.4	5.1 ± 1.5	n.d.

*Only patients with SCC, where figures were given.
†1–2 hr after light meal.
‡Only patients with SCC.
§After overnight fast.
¶200 ml of glucose solution containing 50 g of glucose 1 hr before FDG injection.
**Only lymph node metastases of SCC.
n.g. = not given; n.d. = not done; SUV = standardized uptake value; SCC = squamous-cell carcinoma; FDG = fluorodeoxyglucose.

1 cm and only partial infiltration (Patients 5 and 18) (Table 3). The other 15 patients were classified correctly and, in 32 of 34 neck sides, lymph node involvement was correctly identified. Importantly, all three patients with bilateral malignant lymph nodes (Patients 3, 8 and 17) were correctly assessed. On the basis of involved neck sides, we tried to estimate sensitivity, specificity and positive and negative predictive value and negative predictive value (Table 3). PET revealed 16 true-positive and 16 true-negative neck sides with no false-positive and only two false-negative results. These data result in a sensitivity of 89% and a specificity of 100%. MRI produced 12 false results (7 false-positive and 5 false-negative), with 13 true-positive and 9 true-negative identifications of side involvement, which resulted in a sensitivity of 72% and a specificity of 56%.

Diagnostic Accuracy of Attenuation-Corrected or Nonattenuation-Corrected PET Images for Staging

In nonattenuation-corrected images, a target-to-nontarget activity ratio >2.0 was used as the criterion for malignancy, and the results were compared with those obtained by attenuation-corrected images with a SUV >2.0. In all primary tumors, the SUV and the target-to-nontarget activity ratio were > 2.0. Similar results for N staging were found. One of 41 metastatic lymph nodes was missed by both criteria. The SUV in this lymph node was 1.4, and the target-to-nontarget activity ratio was 1.6. Overall, there was no statistically significant difference between attenuation-corrected and noncorrected images.

DISCUSSION

The predominant type of extracranial tumor found in the head and neck region is SCC. Tumor size and lymph node involvement largely determine the treatment options available to the oncology team (*27*). Previously, clinical evaluation and morphologic imaging procedures were used for preoperative staging. Because of the low specificity of these procedures, however, an improved noninvasive diagnostic workup is needed. With the development of metabolic imaging approaches, tumor tissue can be specifically characterized with tracer techniques.

Fluorine-18-FDG is transported into the cells of most tissues by facilitated diffusion, phosphorylated to FDG-6-PO_4 and trapped intracellularly (*4,28–31*). Because the metabolic pathways of this tracer are relatively well known (*32*), [^{18}F]FDG PET has been extensively used to study glucose metabolism noninvasively in humans (*4*).

Several groups recently reported that there is increased FDG uptake in primary tumors and lymph node metastases in head and neck SCCs (*19–21,23*). The present study confirmed these results and indicated that this cancer could be staged noninvasively with FDG-PET.

Extent of FDG Uptake

In this study population, FDG uptake was extremely variable in primary tumors (SUV 2.0–13.8) and in lymph node metastases (SUV 1.4–11.4). As shown in Table 4, Haberkorn et al. (*20,21*) and Lindholm et al. (*23*) reported similar results with highly variable tracer accumulation. There are several explanations for this heterogeneity. First, it may be due to a partial volume effect, which thus underestimates tracer accumulation in small lesions. As demonstrated in Figure 6, we found no statistically significant correlation between lesion size and FDG uptake. Even if only lesions with a volume <5 ml (which represents a globe with a diameter of about 2 cm) were considered, no

correlation was found. We hypothesized that high FDG uptake in SCCs compensates for the theoretic decrease of signal intensity caused by partial volume effects. The second explanation for the notable variations in SUV in primary tumor and metastases may be the widely accepted concept of cell heterogeneity in human tumors. The primary tumor may consist of a mixture of cell clones, each associated with a different metabolic rate. The hypothesis that lymph node metastases originate from different cell clones may explain why there was no significant correlation between the FDG uptake of the primary tumor and the FDG uptake of lymph node metastases. Finally, the relative contribution of viable tumor cells may vary in the primary tumor and in lymph nodes, which results in a variable mixture of normal, malignant, necrotic and fibrous tissue.

FDG Uptake Kinetics

Another important factor in the assessment of FDG uptake is the time point of its determination. Lindholm et al. (*23*) determined the SUV in their study from 55 to 60 min postinjection, Haberkorn et al. (*20,21,33*) used 60 to 70 min postinjection, and Jabour et al. (*22*) started imaging 30 min postinjection. Time-activity curves for FDG uptake in head and neck SCCs are given by Haberkorn et al. (*20*). They reported an initial maximum about 2 min postinjection followed by a slight decrease and a new increase starting 30 min postinjection. In their study, Minn et al. (*34*) found three different types of FDG time-activity curves. Eight of 13 patients displayed steadily increasing activity; 5 had a level curve with a maximum at 3 min postinjection, followed by a plateau phase; and 6 patients had a decreasing time-activity curve after an early maximum 1 min postinjection. Because both Minn et al. and Haberkorn et al. used 1-min time frames, they were able to detect these early maxima, which probably reflect the effect of tumor blood flow. Only 5-min time frames were used in this study at the beginning of emission scanning, which prohibited evaluation of the time course of tracer uptake during the first minutes. The time-activity curves in the study of Minn et al. (*34*) were recorded only up to 30 min postinjection. During the late uptake period, starting from 30 min postinjection, a steady increase was found in the current study, similar to the results reported by Haberkorn et al. (*20*). Their results and ours indicate that there is no plateau phase up to 60 min postinjection. Because there is a relatively stable tracer concentration in normal tissue over time, static emission scans at later time points may provide higher target-to-nontarget activity ratios. Haberkorn et al. (*20*) did not describe time-activity curves for primary tumors and lymph node metastases. In our study population, we could not find a statistically significant difference in FDG kinetics for tumor and metastases.

Effect of Glucose Plasma Levels

There was no correlation between plasma glucose level and FDG uptake, as shown in Figure 5, which may be due to the exclusion of patients with known diabetes mellitus. All PET examinations were performed after an overnight fast, which resulted in a relatively small range of plasma glucose values. As shown by Wahl et al. (*35*) and Lindholm et al. (*23*), high blood glucose levels decrease FDG uptake in malignant lesions. Diagnostic useful scans might be acquired in diabetic patients, whose blood sugar is well controlled with insulin or other drugs. In ongoing studies, the value of PET imaging for staging of SCC in patients with diabetes mellitus is being investigated.

FDG Uptake and Grading

Several investigators reported a correlation between histologic grading and FDG uptake. Sweeney et al. (*36*) showed in hepatomas that the acceleration of glycolysis corresponds to the tumor's growth rate. Di Chiro et al. (*37*) suggested that glucose metabolic studies may provide an independent measure of the aggressiveness of brain tumors and may supplement pathologic grading. These results were confirmed by other groups (*5,38–40*). In agreement with the results of Haberkorn et al. (*20*), no statistically significant correlation between FDG uptake and grading was observed in SCC of the head and neck region in this study. Nevertheless, there was a trend of higher FDG uptake associated with decreasing cell differentiation, as shown in Figure 7. The lack of a significant correlation might be due to the small patient populations in this study and in that of Haberkorn et al.

FDG-PET for T Staging of SCCs

There is no doubt that "clinical appraisal of the primary tumor alone may not correctly stage the local extent of tumor, since only the mucosal surface is visible" (*27*). Therefore, an accurate tumor staging can only be achieved by the combination of endoscopic evaluation and assessment of deep tissue and nodal involvement by other imaging modalities. Originating from the mucosal surfaces of the upper aerodigestive tract, SCC extend along both the mucosal and deep tissue planes. Ultrasound, CT and MRI have been used for SCC staging (*41–46*). By CT, only 77% (21 of 28) and, by MRI, 81% of the tumors were staged correctly (*47*). In these studies, there were mainly high tumor stages. For correct identification of small tumors (T1), the sensitivity of both methods decreases (only one of three tumors was recognized). Similar results with correct T staging in 80% to 90% of cases have been reported by Glazer et al. (*41*) and Lenz et al. (*48*), who used CT. Steinkamp et al. (*49*) examined 24 patients with laryngeal or hypopharyngeal carcinomas by MRI and endoscopy for preoperative T classification. With respect to tumor classification, MRI was superior for tumor delineation, with correct staging found in 20 of 24 patients (84%); endoscopy only staged 19 of 24 tumors correctly (79%). For higher T stages, this advantage of MRI became more pronounced (only T3 and T4 tumors: MRI, 15 of 16; endoscopy, 12 of 16 correct identifications). On the other hand, endoscopy was superior in small primary tumors (T1 and T2 tumors: MRI, five of eight; endoscopy, seven of eight correct stagings).

Lenz et al. (*50*) reported that panendoscopy staged T levels correctly in only 47% (82 of 174).

Because correct T staging is necessary to define the appropriate surgical approach, these results seem disappointing, and the need for more accurate and reliable methods is well recognized. Eight of 17 patients were overstaged as a result of high uptake in normal mucosa, which has been described by Jabour et al. (*22*), in a study that delineated normal FDG distribution in the head and neck region. This blurring of tumor borders has also been described in contrast-enhanced MRI, because Gd-DTPA tends to migrate in peritumoral, interstitial tissue (*51*).

The overestimation of tumor size by FDG imaging might be avoided by the use of more "restrictive" PET tracers (e.g., labeled amino acids), as they presumably do not show increased tracer uptake in normal mucosa. Leskinen et al. (*52*) reported high ^{11}C-methionine accumulation in head and neck tumors. However, they did not mention whether there was tracer uptake in normal mucosa. Future studies will have to demonstrate possible advantages of alternative tracers. On the other hand, [^{18}F]FDG PET represents a very sensitive method to detect small tumors. All small tumors (five T1 tumors) were identified in the current study; thus, PET may improve staging in patients with positive lymph node involvement and so-called occult primary tumors.

In the future, there might be two other indications for metabolic imaging of primary tumors: (1) if further studies can show the same promising results, as already shown by Haberkorn et al. (*21,33*), [^{18}F]FDG PET might be of use in therapeutic monitoring; and (2) the progress in modern technologies (e.g., overlay techniques) will ease the combination of morphologic and metabolic information. Because both MRI and PET tend to overestimate tumor size, these overlay techniques have to prove their clinical usefulness for T staging in future studies.

FDG-PET for N Staging of SCC of the Head and Neck Region

The detection of nodal metastases at the time of initial presentation affects the choice of treatment and prognosis (*27*). Metastatic disease to lymph nodes decreases the overall survival rate by approximately one half in patients with head and neck cancer (*53*). Accurate preoperative N staging is very important, especially in patients in whom the indication for neck dissection is questioned. In these patients, an N0 classification will influence the therapeutic regimen (*44*). Radiologic and clinical staging of nodes are both limited by their dependence on lymph node size for the diagnosis of malignant lymph node involvement. Up to 30% of cervical lymph node metastases detected by CT or MRI have been missed by the clinical examination (*54, 55*). When done carefully, CT has been shown to alter clinical staging of neck disease in 20% to 30% of patients (*55*). Ultrasound is an inexpensive and practical imaging modality for the evaluation of superficial lymph nodes. If enlarged lymph nodes are regarded as malignant, the sensitivity is high (96%), but specificity as low as 53% has been reported by Gritzmann (*45*).

Lymph node size greater than 1.5 cm or central inhomogeneity (*27*) as criteria for malignant lymph node involvement have been used in CT and MRI. Application of these criteria decreased sensitivity to 92% and raised specificity up to 73% (*45*). Criteria for malignancy, such as central inhomogeneity, however, can only be applied if the size of the lymph node exceeds 1.5 cm (*44*). In histopathologic studies, Eichhorn et al. (*56*) showed that more than 40% of all lymph node metastases are localized in lymph nodes smaller than 1.0 cm, which limits the use of size-dependent criteria. In summary, because of these disappointing results of conventional imaging techniques, some authors suggest that costly examinations such as CT or MRI should not be used for preoperative lymph node staging (*44*).

In the current study, because N stages in subgroups were differentiated according to the TNM system, the results by MRI were correct in only 4 of 17 patients. In addition, we used the size of the lesion as the only criterion for malignancy. These two limitations may have decreased the sensitivity and specificity of MRI in this study for malignant lymph node detection. By [^{18}F]FDG PET, we were able to identify lymph node involvement in 15 of 17 patients correctly. Importantly, we detected the contralateral lymph node involvement in all three patients. The only malignant lymph nodes that were missed by PET were small ipsilateral lymph nodes with diameters of about 1 cm and only partial infiltration. With the criterion, involved neck side, for an estimation of sensitivity and specificity, PET yielded a sensitivity of 89% with only two false-negative results compared with 72% of MRI. PET did not produce false-positive results; MRI reached only a specificity of 56%.

It can be argued that the results of lymph node staging by PET may reflect a selection bias of patients for different kinds of neck dissection. Ipsilateral radical neck dissection was routinely performed in all patients. In contrast, contralateral neck dissection was only performed if suspect lymph nodes were detected preoperatively. For ethical reasons, the preoperative PET results were known to the surgeon, but this altered the decision whether or not to perform a contralateral neck dissection in only one patient. The other nine patients who had contralateral neck dissection had suspect lymph nodes either by CT, MRI or sonography.

CONCLUSION

We used dynamic imaging because we were interested in the kinetics of the FDG uptake. Dynamic imaging protocols over several hours are not suitable for clinical use. Such long examinations will increase the frequency of motion artifacts and, hence, affect the image quality. The examination time can be reduced by restriction of the data

acquisition to emission scans only. Without transmission scans, however, attenuation correction cannot be performed. Therefore, we examined the clinical usefulness of target-to-nontarget activity ratios compared with the calculation of SUV values. We found no statistically significant difference in sensitivity and specificity with nonattenuation-corrected images. These data suggest that, for clinical routine use, an abbreviated protocol with emission scans that delineate FDG distribution in the head and neck region without attenuation correction appears to fulfill all clinical requirements.

ACKNOWLEDGMENTS

We thank E. Zaloudek for excellent technical support in performing the PET studies, the cyclotron and radiochemistry staff for preparing [^{18}F]FDG and Ms. Jodi Neverve for editorial assistance.

REFERENCES

1. Steiner W. Early detection of cancer in the upper aerodigestive tract. Part I. *HNO* 1993;41:360–367.
2. Warburg O. Über den Glukosestoffwechsel der Carcinomzelle. *Klin Wochenschr* 1925;4:534–536.
3. Warburg O, Wind F, Negelein E. On the metabolism of tumors in the body. In: Warburg O, ed., *The metabolism of tumors*. London: Constable; 1930: 254–270.
4. Phelps ME, Huang SC, Hoffman EJ, et al. Tomographic measurement of local cerebral glucose metabolic rate in humans with [F-18] 2-fluoro-2-deoxy-D-glucose: validation of a method. *Ann Neurol* 1979;6:371–388.
5. Alavi JB, Alavi A, Chawluk J, et al. Positron emission tomography in patients with glioma. A predictor of prognosis. *Cancer* 1988;62:1074–1078.
6. Coleman RE, Hoffman JM, Hanson MW, et al. Clinical application of PET for the evaluation of brain tumors. *J Nucl Med* 1991;32:616–622.
7. Di Chiro G. Positron emission tomography using [^{18}F]fluoro-deoxyglucose in brain tumors: a powerful diagnostic and prognostic tool. *Invest Radiol* 1986;22:360–371.
8. Herholz K, Wienhard K, Heiss WD. Validity of PET studies in brain tumors. *Cerebrovasc Brain Metab Rev* 1990;2:240–265.
9. Kim CK, Alavi JB, Alavi A, et al. New grading system of cerebral gliomas using positron emission tomography with F-18 fluorodeoxyglucose. *J Neurooncol* 1991;10:85–91.
10. Rosenfeld SS, Hoffman JM, Coleman RE, et al. Studies of primary central nervous system lymphoma with fluorine-18-fluorodeoxyglucose positron emission tomography. *J Nucl Med* 1992;33:532–536.
11. Rozental JM, Levine RL, Nickles RJ. Changes in glucose uptake by malignant gliomas: preliminary study of prognostic significance. *J Neurooncol* 1991;10:75–83.
12. Valk PE, Budinger TF, Levin VA, et al. PET of malignant cerebral tumors after interstitial brachytherapy. Demonstration of metabolic activity and correlation with clinical outcome. *J Neurosurg* 1988;69:830–838.
13. Gupta NC, Frank AR, Dewan NA, et al. Solitary pulmonary nodules: detection of malignancy with PET with 2-[F-18]-fluoro-2-deoxy-D-glucose. *Radiology* 1992;184:441–444.
14. Kubota K, Matsuzawa T, Fujiwara T, et al. Differential diagnosis of lung tumor with positron emission tomography: a prospective study. *J Nucl Med* 1990;31:1927–1932.
15. Adler LP, Blair HF, Makley JT, et al. Noninvasive grading of musculoskeletal tumors using PET. *J Nucl Med* 1991;32:1508–1512.
16. Bares R, Klever P, Hellwig D, et al. Pancreatic cancer detected by positron emission tomography with ^{18}F-labeled deoxyglucose: method and first results. *Nucl Med Commun* 1993;14:596–601.
17. Wahl RL, Cody RL, Hutchins GD, et al. Primary and metastatic breast carcinoma: initial clinical evaluation with PET with the radiolabeled glucose analogue 2-[F-18]-fluoro-2-deoxy-D-glucose. *Radiology* 1991;179:765–770.
18. Minn H, Soini I. Fluorine-18-fluorodeoxyglucose scintigraphy in diagnosis and follow up of treatment in advanced breast cancer. *Eur J Nucl Med* 1989;15:61–66.
19. Reisser C, Haberkorn U, Strauss LG. PET scan in tumor diagnosis in the head and neck. *Laryngorhinootologie* 1991;70:214–217.
20. Haberkorn U, Strauss LG, Reisser C, et al. Glucose uptake, perfusion, and cell proliferation in head and neck tumors: relation of positron emission tomography to flow cytometry. *J Nucl Med* 1991;32:1548–1555.
21. Haberkorn U, Strauss LG, Dimitrakopoulou A, et al. Fluorodeoxyglucose imaging of advanced head and neck cancer after chemotherapy. *J Nucl Med* 1993;34:12–17.
22. Jabour BA, Choi Y, Hoh CK, et al. Extracranial head and neck: PET imaging with 2-[F-18]fluoro-2-deoxy-D-glucose and MR imaging correlation. *Radiology* 1993;186:27–35.
23. Lindholm P, Minn H, Leskinen-Kallio S, et al. Influence of the blood glucose concentration on FDG uptake in cancer—a PET study. *J Nucl Med* 1993;34:1–6.
24. Hamacher K, Coenen HH, Stöcklin G. Efficient stereospecific synthesis of no-carrier-added 2-[^{18}F]-fluoro-2-deoxy-D-glucose using aminopolyether supported nucleophilic substitution. *J Nucl Med* 1986;27:235–238.
25. Hermanek P, Sobin LH, *TNM classification of malignant tumors*, 4th edition, 2nd revision. New York: Springer-Verlag; 1992.
26. Hoffmann H. *Formelbuch: formeln mathematik. langenscheidts formelbücher*. München: Langenscheidt KG; 1985.
27. Dillon WP, Harnsberger HR. The impact of radiologic imaging on staging of cancer of the head and neck. *Semin Oncol* 1991;18:64–79.
28. Sokoloff L, Reivich M, Kennedy C, et al. The [^{14}C]deoxyglucose method for the measurement of local cerebral glucose utilization: theory, procedure, and normal values in the conscious and anesthetized albino rat. *J Neurochem* 1977;28:897–916.
29. Som P, Atkins HL, Bandoypadhyay D. A fluorinated glucose analog, [^{18}F] 2-fluoro-2-deoxy-D-glucose: nontoxic tracer for rapid tumor detection. *J Nucl Med* 1980;21:670–675.
30. Besell EM, Thomas P. The effect of substitution at C-2 of D-glucose 6-phosphate on the rate of dehydrogenation by glucose 6-phosphate dehydrogenase (from yeast and from rat liver). *Biochem J* 1973;131:83–89.
31. Coe EL. Inhibition of glycolysis in ascites tumor cells preincubated with 2-deoxy-2-fluoro-D-glucose. *Biochim Biophys Acta* 1972;264:319–327.
32. Reivich M, Alavi A, Wolf A. Glucose metabolic rate kinetic model parameter determination in humans: the lumped constants and rate constants for [^{18}F]fluorodeoxyglucose and [^{11}C]deoxyglucose. *J Cereb Blood Flow Metab* 1985;5:179–192.
33. Haberkorn U, Reinhardt M, Strauss LG, et al. Metabolic design of combination therapy: use of enhanced fluorodeoxyglucose uptake caused by chemotherapy. *J Nucl Med* 1992;33:1981–1987.
34. Minn H, Paul R, Ahonen A. Evaluation of treatment response to radiotherapy in head and neck cancer with fluorine-18 fluorodeoxyglucose. *J Nucl Med* 1988;29:1521–1525.
35. Wahl RL, Henry CA, Ethier SP. Serum glucose: effects on tumor and normal tissue accumulation of 2-[F-18]-fluoro-2-deoxy-D-glucose in rodents with mammary carcinoma. *Radiology* 1992;183:643–647.
36. Sweeney MJ, Ashmore J, Morris HP. Comparative biochemistry of hepatomas. IV. Isotope studies of glucose and fructose metabolism in liver tumors of different growth rates. *Cancer Res* 1963;23:995–1002.
37. Di Chiro G, De LaPaz R, Brooks R. Glucose utilization of cerebral gliomas measured by [^{18}F]fluorodeoxyglucose and positron emission tomography. *Neurology* 1982;32:1323–1329.
38. Di Chiro G, Hatazawa J, Katz DA, et al. Glucose utilization by intracranial meningiomas as an index of tumor aggressivity and probability of recurrence: a PET study. *Radiology* 1987;164:521–526.
39. Kornblith PL, Cummins CJ, Smith GH, et al. Correlation of experimental and clinical studies of metabolism by PET scanning. *Prog Exp Tumor Res* 1984;27:170–178.
40. Mineura K, Yasuda T, Kowada M. Positron emission tomographic evaluation of histological malignancy in gliomas using oxygen-15 and fluorine-18-fluorodeoxyglucose. *Neurol Res* 1986;8:164–168.
41. Glazer H, Niemeyer JH, Blafes DM. Neck neoplasms: MRI imaging part I. Initial evaluation. *Radiology* 1986;160:343–348.
42. Sagerman R, Chung C. Computed tomography in management in head and neck cancer. *Computed Tomography* 1983;5:229–235.
43. Som P. Lymph nodes of the neck. *Radiology* 1987;165:593–600.
44. Quetz JU, Rohr S, Hoffmann P, et al. B-image sonography in lymph node staging of the head and neck area. A comparison with palpation, computerized and magnetic resonance tomography. *HNO* 1991;39:61–63.
45. Gritzmann N. Imaging procedures in diagnosis of laryngeal cancer with special reference to high resolution ultrasound. *Wien Klin Wochenschr* 1992;104:234–242.
46. Gatenby RA, Mulhern CJ, Strawitz J, et al. Comparison of clinical and computed tomographic staging of head and neck tumors. *Am J Neuroradiol* 1985;6:399–401.

47. Steinkamp HJ, Maurer J, Heim T, et al. Magnetic resonance tomography and computerized tomography in tumor staging of mouth and oropharyngeal cancer. *HNO* 1993;41:519–525.
48. Lenz M, Bongers H, Ozdoba C, et al. Klinische Wertgkeit der Computertomographie beim prätherapeutischen T-Staging von orofazialen Tumoren. *Rofo Fortschr Geb Rontgenstr Neuen Bildgeb Verfahr* 1989;151:138–144.
49. Steinkamp HJ, Heim T, Zwicker C, et al. The value of nuclear magnetic resonance tomography in tumor staging of laryngeal-/hypopharyngeal cancer. *HNO* 1992;40:339–345.
50. Lenz M, Skalej M, Ozdoba C, et al. Kernspintomographie der Mundhöhle und des Mundbodens: Vergleich mit der Computertomographie. *Rofo Fortschr Geb Rontgenstr Neuen Bildgeb Verfahr* 1989;150:425–433.
51. Wagner-Manslau C, Bauer R, van de Flierdt E, et al. Wertigkeit von SE-, IE- und GE-Sequenzen bei Tumoren im Kopf-Hals-Bereich. *Rofo Fortschr Geb Rontgenstr Neuen Bildgeb Verfahr* 1990;153:154–160.
52. Leskinen KS, Nagren K, Lehikoinen P, et al. Carbon-11-methionine and PET is an effective method to image head and neck cancer. *J Nucl Med* 1992;33:691–695.
53. Batsakis JG. *Tumors of the head and neck: clinical and pathological considerations*. Baltimore: Williams & Wilkins; 1984.
54. Mancuso AA, Maceri D, Rice D. CT of cervical lymph node cancer. *Am J Roentgenol* 1981;136:381–385.
55. Stevens MH, Harnsberger HR, Mancuso AA, et al. Computed tomography of cervical lymph nodes. Staging and management of head and neck cancer. *Arch Otolaryngol* 1985;111:735–739.
56. Eichhorn T, Schroeder HG, Glanz H, et al. Histologisch kontrollierter Vergleich von Palpation und Sonographie bei der Diagnose von Halslymphknotenmetastasen. *Laryngol Rhinol Otol* 1987;66:266–274.

CORRECTION

In the August issue of *JNM*, the article, "Differentiation of Infected from Noninfected Rapidly Progressive Neuropathic Osteoarthropathy," by D. S. Schauwecker, incorrectly stated two patients as having foot disease and metacarpal destruction. The correct wording should be foot disease and metatarsal destruction.